Viruses Masquerading as Antibodies in Biosensors: The Development of the Virus BioResistor

Apurva Bhasin[1], Nicholas P. Drago[1],Sudipta Majumdar[1], Emily C. Sanders[1], Gregory A. Weiss[1,2,3]*, Reginald M. Penner[1]*

[1]*Department of Chemistry, University of California, Irvine, Irvine, CA 92697*
[2]*Department of Pharmaceutical Sciences, University of California, Irvine, Irvine, CA 92697*
[3]*Department of Molecular Biology & Biochemistry. University of California, Irvine, Irvine, CA 92697*

Address correspondence to: gweiss@uci.edu, rmpenner@uci.edu.

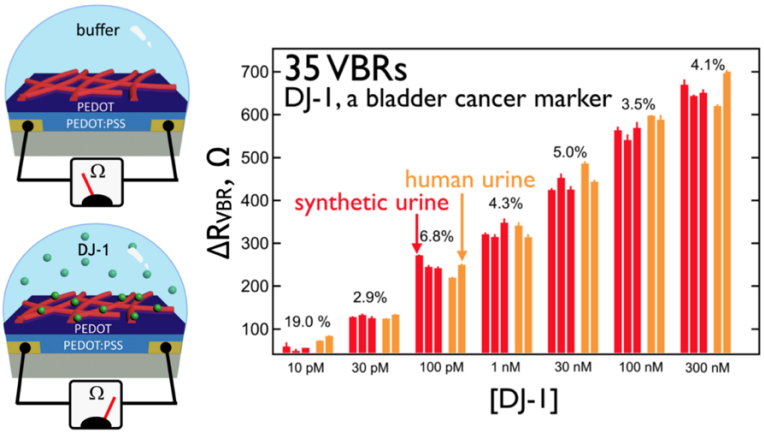

Conspectus:

The 2018 Nobel Prize in Chemistry recognized *in vitro* evolution, including the development by George Smith and Gregory Winter of phage display, a technology for engineering the functional capabilities of antibodies into viruses. Such bacteriophage solve inherent problems with antibodies including their high cost, thermal lability, and their propensity to aggregate. While phage display accelerated the discovery of peptide and protein motifs for recognition and binding to proteins in a variety of applications, the development of biosensors using intact phage particles was largely unexplored in the early 2000's. Virus particles, 16.5 MDa in size and assembled from thousands of proteins, could not simply be substituted for antibodies in any existing biosensor architectures.

Incorporating viruses into biosensors required us to answer several questions: What process will allow the incorporation of viruses into a functional bioaffinity layer? How can the binding of a protein disease marker to a virus particle be electrically transduced to produce a signal? Will the variable salt concentration of a bodily fluid

interfere with electrical transduction? A completely new biosensor architecture, and a new scheme for electrically transducing the binding of molecules to viruses, was required.

This Account describes the highlights of a research program, launched in 2006, that answered these questions. These efforts culminated in 2018, in the invention of a biosensor specifically designed to interface with virus particles – the *Virus BioResistor (VBR).* The *VBR* is a resistor, consisting of a conductive polymer matrix into which M13 virus particles are entrained. The electrical impedance of this resistor, measured across four orders of magnitude in frequency, simultaneously measures the concentration of a target protein and the ionic conductivity of the medium in which the resistor is immersed. Large signal amplitudes coupled with the inherent simplicity of the VBR sensor design results in high signal-to-noise (S/N >100) and excellent sensor-to-sensor reproducibility. Using this new device, we have measured the urinary bladder cancer biomarker, nucleic acid deglycase (DJ-1) in urine samples. This optimized VBR is characterized by extremely low sensor-to-sensor coefficients-of-variation in the range of 3-7% across the DJ-1 binding curve down to a 30 pM limit-of-quantitation (LOQ), encompassing four orders of magnitude in concentration.

Key References:

- Yang, L. M. C.; Tam, P. Y.; Murray, B. J.; McIntire, T. M.; Overstreet, C. M.; Weiss, G. A.; Penner, R. M. Virus Electrodes for Universal Biodetection. *Anal. Chem.* **2006**, *78*, 3265–3270. *Our first biosensor exploiting immobilized virus particles, instead of antibodies, as receptors.*[1]
- Donavan, K. C.; Arter, J. A.; Weiss, G. A.; Penner, R. M. Virus-Poly(3,4-Ethylenedioxythiophene) Biocomposite Films. *Langmuir* **2012**, *28*, 12581–12587. *First description and characterization of the electrodeposition of virus-PEDOT composite films.*[2]
- Bhasin, A.; Ogata, A. F.; Briggs, J. S.; Tam, P. Y.; Tan, M. X.; Weiss, G. A.; Penner, R. M. The Virus Bioresistor: Wiring Virus Particles for the Direct, Label-Free Detection of Target Proteins. *Nano Lett.* **2018**, *18*, 3623–3629. *The first paper describing the Virus BioResistor (VBR).*[3]
- Bhasin, A.; Sanders, E. C.; Ziegler, J. M.; Briggs, J. S.; Drago, N. P.; Attar, A. M.; Santos, A. M.; True, M. Y.; Ogata, A. F.; Yoon, D. V; Majumdar S.; Wheat, A. J.; Patterson, S. V., Weiss, G. A.; Penner, R. M., Virus Bioresistor (VBR) for Detection of Bladder Cancer Marker DJ-1 in Urine at 10 PM in One Minute. *Anal. Chem.* **2020**, *92*, 6654–6666. *First demonstration of detection, at 10 pico-molar concentrations, of a cancer marker in human urine using the VBR.*[4]

I. Introduction.

In 2020, the most reliable techniques used by doctors for cancer surveillance are identical to practices from twenty years ago: colonoscopy (colon cancer), mammogram (breast cancer), and Pap smear (cervical cancer). Cancer surveillance involving the analysis of blood and urine for cancer markers – so called liquid biopsies - are not part of an annual physical examination for most Americans because biosensors and laboratory assays that facilitate rapid, reliable, and affordable analyses for cancer markers do not yet exist.

We became interested in this problem in 2005.[1] Up to this time, most biosensors designed to detect the distinctive protein "biomarkers" produced by cancers used antibodies to recognize and bind these proteins. M13, a filamentous bacteriophage that infects Ecoli, was engineered to "display" Fv antibody fragments on their surfaces providing an intriguing opportunity for the development of cheaper, more robust biosensors. The basic approach for the "display" of proteins on the M13 phage surface was invented by George Smith in 1985,[5,6] before Jim Wells and co-workers introduced key and necessary improvements to enable Greg Winter to display an antibody, or Fv, on the phage surface.[7,8] Our labs exploited these seminal contributions to extend phage display into biosensing applications.

M13 viruses are an attractive alternative to antibodies in biosensors for three main reasons: 1) the cost of engineered viruses is much lower, 2) the affinity of virus particles is similar (often dissociation constants, K_D, are below 10^{-9} M), and, 3) virus particles are quite robust, and, for example, do not require refrigeration to maintain potency. In principle, biosensors based upon virus particles could be cheaper to manufacture and cheaper to distribute and store, especially in the resource-challenged third world. In this Account, we trace the development over fourteen years of a new biosensor, the *Virus BioResistor* or *VBR*[4,3], designed specifically for rapid (60 s), point-of-need detection of cancer markers in urine using virus receptors.

II. Virus biosensors that Resemble Antibody Biosensors

a. A Covalent Virus Layer (CVL). A generic biosensor has three components: i) A *bioaffinity layer* equipped with receptors, such as ss-DNA probes or antibodies to recognize and to bind a target DNA or protein, respectively, ii) a *transducer* that detects the binding of the target to the bioaffinity layer using a measurement of properties such as the mass of this layer, or its optical or electrical response, and, iii) *electronics* that convert the raw transducer signal into a quantitative measure of the target concentration.

Bioaffinity layers for the detection of proteins have often exploited monolayers of antibodies conjugated to polymer or glass surfaces.[9] The first biosensors to exploit the Nobel Prize-winning phage-display technologies[7,8,5,6] were demonstrated in 2003 by a team at Auburn University lead by Valery Petrenko and Vitaly Vodyanoy.[10] In that work, M13 virus particles were immobilized by physisorption onto the surface of an acoustic wave sensor and used to measure the binding of β-galactosidase, a 465 kDa protein, at concentrations down to 0.60 nM.[10] These experiments provided the first proof-of-concept that viruses could function as receptors in biosensors. However, physisorbed virus layers,[10–12] were unstable in our measurements, compromising

precision.

Li-Mei Yang, working with Juan Diaz and Phillip Tam, attempted to remedy the stability problem by preparing monolayers of M13 virus particles that were covalently bonded to a gold electrode surfaces (Figure 1).[13,14] Her approach was to first electrochemically roughening a gold electrode, before exposing it to thioctic NHS ester to form a thiol−Au bonded self-assembled monolayer or SAM and then treating the SAM with a suspension of virus particles thereby forming a covalent amide bond between free amines on the phage coat peptide and the activated carboxylate at the surface of the SAM. The final step was to plug any defects in this "covalent virus layer" (CVL) with bovine serum albumin (BSA) to minimize nonspecific adsorption (Figure 1a, step 3). The CVL is complete after Step 3. Steps 4, 5 and 6 in Figure 1 illustrate the reversible binding of p-Ab by the CVL.

Atomic force microscopy (AFM)[13,14] showed that the CVL consists of a close-packed monolayer of filamentous M13 virus particles (Figure 1b). When many M13 virus are covalently bound to a surface, the densely packed "monolayer" of the virus resembles a shag carpet (Figure 1a). The resulting CVL retains significant free volume as evidenced by the fact that each phage particle is capable of binding 140 antibodies to the p8 majority coat peptide (p8-Ab, 148 kDa), on average.[13] In the vacuum of a scanning electron microscope (SEM), the water and ions supporting the shag carpet are removed and filamentous virus particles collapsed onto the surface can be clearly seen (Figure 1d).

b. Mass-Based Signal Transduction of the CVL.

The properties of the CVL for biosensing were first explored in 2008. Both mass-based biosensing,[13] conducted by depositing the CVL on a gold quartz-crystal microbalance (QCM) transducer, and electrochemically-based sensing[14] were evaluated. In these experiments, the response of a CVL-modified gold surface to p8-Ab was studied.[13,14]

To measure the mass responses of a CVL during exposure of p8-Ab, the QCM crystal was mounted in a Teflon flow cell that provided for the radially symmetric delivery of solution to the circular QCM electrode surface (Figure 2a,b).[13] The increase in mass observed upon p8-Ab exposure (≈3 μg/cm^2) could be reversed by washing briefly with aqueous acid (Figure 2c), enabling mass *versus* [p8-Ab] calibration data to be acquired over a wide range of [p8-Ab] for a single CVL (Figure 2d-f). These data were linear from 6.6 nM to 200 nM p8-Ab.[13] A non-binding antibody (n-Ab) control showed negligible non-specific signal over this concentration range, establishing the limit-of detection for p8-Ab as 20 nM. These data demonstrated that virus particles within the CVL were available for the rapid binding of antibody, suggesting that the CVL could function as a bioaffinity layer within a biosensor. These data demonstrated that p8-Ab binding, while reversible, exhibited a very slow off-rate of $<10^{-5}$ s^{-1}, indicating that re-use of the CVL.[13] The next question was: Can the binding of a target antibody be detected using the electrochemical response of these virus-modified electrodes instead of a QCM?

c. Electrochemical Signal Transduction of the CVL.

In addition to mass-based transduction using QCM[13], the electrochemical response of the CVL to p8-Ab and n-Ab were investigated using electrochemical impedance spectroscopy (EIS).[14] A goal in these experiments was to carry out *direct detection* of antibody binding to the CVL. "Direct" in this context meant that a redox couple such as $Fe(CN)_6^{4-/3-}$ was not added to the testing solution, an "*indirect*" approach in which the blocking of Faradaic electron transfer signal protein binding to an electrode surface.[15–20] Direct EIS measurements, in contrast, probed changes to the non-Faradaic impedance of the CVL-modified gold electrode caused by antibody binding to the surface.

A surprising conclusion of these experiments was that the highest signal-to-noise (S/N ≈ 20) and best selectivity for p8-Ab binding to the CVL-modified electrode occurred at high frequencies in the range from 4 kHz – 140 kHz, in spite of the fact that the shift in the real component of the impedance signal, ΔZ_{re}, was the smallest in this frequency range – with $\Delta Z_{re} < 10\ \Omega$ at all p8-Ab concentrations.[14] Selectivity for p8-Ab versus n-Ab was completely lost at lower frequencies, where ΔZ_{re} signals as large as 1 kΩ were observed. In contrast, prior work on EIS-detected indirect biosensors had emphasized the detection of target proteins at low frequencies, below 5 Hz in most cases. Z_{re} is increased by p8-Ab binding to the CVL because the bound, insulating p8-Ab molecules displace ionically conductive electrolyte from the free volume within the CVL layer.[14] The LOD for p8-Ab in these experiments, limited by the low ΔZ_{re} signal amplitude, was 20 nM.[14]

The conclusion from these experiments was that this CVL did not afford enough sensitivity to enable the detection of proteins at sub-nM concentrations, as required for cancer screening. A fundamentally new method for preparing a virus-based bioaffinity layer was needed.

III. Virus-PEDOT Bioaffinity Layers

a. Electrodepositing a Virus-PEDOT Composite Film.

Inspiration for a new type of virus-based bioaffinity layer arrived from an unexpected direction. In the 2010 time frame, the Penner group had been investigating the thermoelectric properties of nanowires composed of the electronically conductive organic polymer PEDOT (poly(3,4-ethylene dioxythiophene).[21] These PEDOT nanowires were prepared by electrodeposition, using the Lithographically Patterned Nanowire Electrodeposition (LPNE) method.[22,23]

Could PEDOT act as a host for M13 virus particles? This idea was interesting for two reasons: First, the electronic conductivity of PEDOT provided a means by which biosensor signal from M13 particles could be directly transmitted to an external circuit. Second, PEDOT is positively charged as synthesized, with one positive charge for each 4 or 5 EDOT residues. During electropolymerization (Figure 3a), 3,4-ethylene dioxythiophene (EDOT) is oxidized to a cation radical, and radical coupling occurs near the electrode surface until the resulting oligomers lose solubility and, with anions from the solution to balance the positive charge, they precipitate onto the electrode. M13 virus particles have a net negative charge near 6000, as a consequence of three ionizable moieties, Glu2, Asp4 and Asp5, on the 2700 copy P8 majority coat protein near its exposed N-terminus.[24] Our hypothesis was that the

polymerization of positively-charged PEDOT in the presence of negatively charged M13 would electrostatically promote the incorporation of M13 particles within the polymer matrix.

To test this hypothesis, virus-PEDOT biocomposite films were prepared by electropolymerizing EDOT in aqueous electrolytes containing just 12 mM $LiClO_4$ and nM concentration of M13 virus particles.[2] In these experiments, it was observed that the virus concentration was increased from 3 to 15 nM (the solubility limit), the EDOT electropolymerization current peak was depressed as compared to the virus-free control.[2] This observation suggested that the virus particles were either interfering with, or participating in, EDOT polymerization. QCM gravimetry (Figure 3b) showed that the mass of the resulting films was augmented when virus particles were present in the EDOT polymerization solution. The excess mass, relative to pure PEDOT films (Figure 3c), was attributed to the incorporation of virus particles into the growing PEDOT film.[2] This observation directly demonstrated that virus particles were being incorporated into these electrodeposited PEDOT films, as predicted by the reaction of Figure 3a.

How efficient is the virus incorporation into these films during electropolymerization? The QCM data of Figure 3c provided the answer: The difference in mass (the vertical axis) at a particular deposition charge, Q_{tot}, could be attributed to virus incorporated into the virus-PEDOT composite film. This analysis showed that concentration of the M13 in the virus-PEDOT film prepared by electrodeposition was directly proportional to the M13 concentration in the polymerization solution (Figure 3d), and the slope of this line was an astonishing ≈500. These experiments demonstrated that the reaction shown in Figure 3a provided for highly efficient incorporation of virus into a growing PEDOT film. SEM images of electrodeposited virus-PEDOT composite films showed a striking transformation as virus was incorporated into the plating solution (Figure 3e-j). In these images, bundles of virus particles are seen protruding at the surface of the virus-PEDOT films, and as expected, the density of these virus particles is correlated with the concentration of virus in the deposition solution.[2]

b. Biosensing with Virus-PEDOT Nanowires.

What would be the best way to exploit this new virus-PEDOT material in a biosensor? Our initial answer to this question was to prepare arrays of nanowires composed of virus-PEDOT.[25,26] These were prepared using LPNE[22,23,27] in conjunction with the same electrodeposition protocol employed for virus-PEDOT films described above.[2] The resulting virus-PEDOT nanowires, deposited onto glass surfaces, were linear, millimeters in length, ≈300 nm in width and 60 nm in height. SEM, AFM and fluorescence microscopy confirmed the incorporation of M13 into the conducting PEDOT nanowire arrays, and further fluorescence studies also demonstrated the viruses remained intact and fully functional for binding to analytes.[25,26]

Biosensing experiments were conducted by measuring the dc resistance of a virus-PEDOT nanowire array, rather than the frequency-dependent impedance of these arrays,[25,26] as in previous studies, and p8-Ab and the n-Ab control were compared as before. A p8-Ab concentration dependent increase in resistance was

observed, culminating in a 40% increase in response to exposure to 99 nM buffered p8-Ab solutions. A limit-of-detection for p8-Ab of 20 nM was established for these nanowire arrays. n-Ab showed no measurable signal.[25]

Arrays of virus-PEDOT nanowires were also employed for the detection of prostate-specific membrane antigen (PSMA), a promising urine-borne cancer marker for prostate cancer.[28,29] PSMA is a 750 residue, 100 kDa glycoprotein that is overexpressed as a homodimer on the surface of prostate cancer cells.[28,29] These studies exploited virus particles engineered to display the PSMA-binding epitope PSMA-3 (amino acid sequence SECVEVFQNSCDW). In spite of this change to the virus, the virus-PEDOT electrodeposition is unaffected because this process is completely modular with respect to the phage incorporation. In spite of the smaller size of PSMA relative to antibodies (100 kDa *versus* 155 kDa), similar detection metrics were achieved in this study which culminated in a LOD_{PSMA} of 66 nM in high salt (≈160 mM) PBS buffer solutions and a linear response up to 150 nM PSMA.

The conclusion of these two studies[25,26] was that arrays of virus-PEDOT nanowires performed approximately as well as the EIS-transduced CVL-modified gold electrodes. A more direct comparison of virus-PEDOT with the CVL was needed in experiments that exploited conventional electrodes and EIS, and this was our next step.

c. Electrochemical Signal Transduction for virus-PEDOT films.

As compared with virus-PEDOT nanowires, a simpler approach was to coat a virus-PEDOT film onto a gold electrode. The response of such electrodes was studied using EIS for the detection of PSMA[30,31] and, separately, p8-Ab.[32] p8-Ab detection at virus-PEDOT electrodes showed much higher signal-to-noise, ranging from 17 to 30, at high frequencies in the 100 Hz – 10 kHz range. At 1 kHz, a LOD for p8-Ab of 6 nM was achieved, and quantitation of p8-Ab up to 65 nM was possible. This represented a 65% reduction in LOD for p8-Ab compared to the identical experiment conducted using CVL-modified gold electrodes.

An even better result was obtained for the detection of PSMA using a new paradigm: Synergistic dual ligand phage.[30,31] The hypothesis tested in this paper was that two peptide binders are better than one. In other words, the sensitivity to PSMA could be improved by incorporating a *second* peptide binder (called *KCS-1*) for PSMA onto an engineered phage (phage-2) that already displayed a peptide binder for the protein (Figure 4a). This was accomplished by conjugating a positively charged poly(lysine) tether to the polypeptide and then permitting it to self-assemble by electrostatic attraction onto the negatively charged phage after the electrodeposition of virus-PEDOT bioaffinity layer (Figure 4b).[30,31] The addition of the second ligand, KCS-1, significantly increased the affinity of the virus for PSMA in ELISA measurements (data not shown), and for electrochemical measurements (Figure 4d). This enhanced sensitivity afforded a LOD_{PSMA} = 100 pM was seen both in buffer and in synthetic urine solutions (Figure 4e) for these dual ligand systems.

IV. The Virus BioResistor.

a. **The two-sided virus-PEDOT biosensor** – All of the virus-based biosensors investigated in our laboratories up to 2015 were laboratory experiments[1,4,13,14,25,26,30,32,33] in the sense that electrochemical measurements conducted using three-electrode cells incorporating separate reference, counter, and working (sensor) electrodes. A portable, miniaturizable, and commercializable electrochemical sensor architecture – in which the necessary electrodes were incorporated into a single monolithic sensor body - had not been demonstrated.

This advance occurred in 2017 with the demonstration by Alana Ogata, Ming Tan, and others that two virus-PEDOT modified gold electrodes, without reference or counter electrodes (Figure 5a), could function as a biosensor for human serum albumin (HSA).[34] Prior work on PSMA[31,33] had demonstrated that the signal generated by a virus-PEDOT-modified gold electrode was concentrated in the resistive component of the impedance, Z_{re}, instead of the capacitive component, Z_{im}. The hypothesis explored in the 2017 "two-sided" sensor architecture (Figure 5b) was that arranging *two* virus-PEDOT bioaffinity layers electrically in series would double the impedance signal produced by the biosensor.[34]

In spite of its simplicity, the two-sided virus-PEDOT biosensor reliably distinguished HSA from BSA – proteins of identical size and having a 76% sequence homology. This demonstrated that the inherent selectivity of the engineered virus could be recovered with this device (Figure 5b,c). At an optimized detecting frequency of 340 Hz (Figure 5d), the two-sided sensor produced a prompt increase in Z_{re} within 5 s and a stable Z_{re} signal within 15 min. HSA concentrations in the range from 100 nM to 5 μM were detectable (Figure 5e). These single-use biosensors demonstrated excellent sensor-to-sensor reproducibility characterized by a coefficient-of-variation of 2−8% across the entire concentration range.[34] Two-sided virus-PEDOT sensors in synthetic urine demonstrated a concentration dependent response to HSA similar to PBS buffer.

This performance provided reason for optimism, however the two-sided virus-PEDOT biosensor had two serious deficiencies: First, its 100 nM LOD for HSA was insufficient to measure cancer markers in urine at sub-nanomolar concentrations. The two-sided sensor simply didn't produce enough signal - a *maximum* of 12 Ω of signal against a 100-200 Ω background (Figure 5e).[34] Second, the two-sided biosensor required that current was carried through the test solution between the two electrodes, thus convoluting the resistance change due to binding of the target protein with the resistance of the solution. Since urine and other bodily fluids have highly variable ionic conductivities, this imposes a barrier to the clinical use of this biosensor. In order to provide reliable results for highly variable single patient samples, a biosensor architecture that decoupled target binding from ionic conduction was required. On spite of these two issues, the two-sided virus-PEDOT biosensor was the progenitor of the VBR.

b. **The Virus BioResistor (VBR)** – Alana Ogata and Apurva Bhasin collaborated to invent the VBR in 2017, and since then, to fully realize its capabilities.[3,4] The extension of the two-sided biosensor to the VBR is almost trivial: The virus-PEDOT

bioaffinity layer was extended across the gap between the two gold electrodes. Since the virus-PEDOT layer is electrodeposited, this modification required that a conductor was deposited across this gap first. A spin-coated PEDOT layer was used for this purpose and the virus-PEDOT layer was electrodeposited on top of it (Figure 6a,b).[3,4] We refer to this two-layer construct connecting the gold electrodes as the VBR "channel". This elaboration of the two-sided biosensor dramatically alters its properties.

When the two gold electrodes are directly connected via the channel, an internal circuit is generated for the VBR (Figure 6c) in which the resistance of the channel is arranged in parallel with the series capacitance and the resistance of the solution. This circuit produces a distinctive semicircular Nyquist (Z_{im} vs. Z_{re} as a function of frequency) plot that can be modeled with two equations:[3,4]

$$-Zim = \frac{\omega C_{\mathrm{vbr}} R_{\mathrm{VBR}}^2}{1 + \omega^2 C_{\mathrm{vbr}}^2 (R_{\mathrm{sol}} + R_{\mathrm{VBR}})^2}$$

$$Zre = \frac{R_{\mathrm{VBR}}(1 + \omega^2 C_{\mathrm{vbr}}^2 R_{\mathrm{sol}}(R_{\mathrm{sol}} + R_{\mathrm{VBR}}))}{1 + \omega^2 C_{\mathrm{vbr}}^2 (R_{\mathrm{sol}} + R_{\mathrm{VBR}})^2}$$

In contrast, the Nyquist plot for a two-sided biosensor produces a linear plot (Figure 5c). The response of three VBRs to the protein DJ-1, a bladder cancer (BC) biomarker,[35,36] shows increasing diameter for the semicircle (Figure 6d). This increase in diameter is produced by a shift in the low frequency Z_{re} to higher values, while the high frequency edge of the semicircle is unchanged. This shift in the low frequency Z_{re} correlates with the concentration of target protein. One consequence of this circuit, shown in the signal-to-noise *versus* frequency plot (Figure 6e), is that the S/N ratio peaks at low frequency (≈ 1 Hz) and is negligible above 100 Hz. The high frequency edge of the semicircle measures the solution resistance, R_{soln}. We have demonstrated[3] that these two resistors, R_{VBR} and R_{soln} are orthogonal, allowing the value of R_{VBR} to be accurately measured independent of the value of R_{soln}. This means that the ionic resistance of the test solution does not interfere with accurate measurement of the concentration of target protein – a critically important capability for clinical measurements.

The potential of the VBR for the detection of bladder cancer in urine is supported by the data of Figure 7.[4] Here, a calibration curve for the detection of DJ-1, a 20 kDa BC marker[35,36] in both synthetic and human urine is shown (Figure 7a,b), comprised of data acquired from 35 individuals VBRs. These data demonstrate a lower LOD of 10 pM for DJ-1, as well as a sensor-to-sensor coefficient of variation of <7% across the DJ-1 binding curve, spanning 4 orders of magnitude, down to 30 pM. [4] Selectivity for DJ-1 (Figure 7c) is also excellent and is achieved without the use of any blocking agent (e.g., casein or BSA).[4] The signals plotted in Figure 7a,b are all measured after a brief one minute exposure to DJ-1-spiked urine (Figure 7d).[4] But a useful benchmark, the concentrations of DJ-1 in the urine of healthy and BC-positive patients, has not yet been established.[35,36]

The mechanism by which the VBR operates remains under investigation, but a working hypothesis is summarized by Figure 7e,f.[4] Evidence suggests that the

affinity-driven diffusion of target protein into the virus-PEDOT layer produces an increase in its low-frequency impedance. This impedance increase may be caused by the disruption of inter-chain electrical contacts between PEDOT chains in this material. Further experimentation, now underway, will be required to either refute or confirm this hypothesis.[4]

c. **Biosensor Architectures Related to the VBR -** How does the VBR architecture and capabilities compare with other biosensors? The closest relative of the VBR is the organic electrochemical transistor (OECT).[37–39] OECTs generally have a reference electrode, in addition to source and drain electrodes, and a semi-conducting polymer film channel, similar to the VBR. The device is immersed in an electrolytic solution, the source and drain are bridged by the polymer, and the reference electrode placed in the same electrolytic solution. By biasing one of the electrodes at a set potential the doping level of the polymer would change, inducing a large conductivity change. At the same time, the potential at another electrode would be swept and the current at the third electrode would be measured. This allowed for small changes in the doping level of the film to be measured with great accuracy.[37] By conjugating a bio-recognition element to the polymer film, low LODs (1 nM) and high specificity have been achieved for label-free detection of proteins.[40]

While OECTs can achieve detection of many analytes, these devices have limitations when it comes to clinical biomolecular sensing. High ionic strength solutions cause Debye screening and prevent low LODs.[41] The doping level of the polymer is dependent on the ions in the solution, which can cause issues when ion detection is not desired.[39]

V. Summary and Outlook.

The VBR is noteworthy for its extreme simplicity, for its use of virus particles in place of antibodies as receptors, and because it's performance for the detection of some cancer markers directly on bodily fluids can be adequate for the early detection of cancer. The 14 year story of its development, recounted here, includes both dead-ends (two-sided biosensors) and near failures (nanowires). That it now exists is a testament to the power of perseverance in science.

A future goal is to create arrays of VBRs in which each VBR element contains a different M13 virus particle capable of detecting a different cancer or disease marker. Such a proteomic panel might provide a multi-dimensional picture containing information on disease progression and tumor grade.

BIOGRAPHICAL INFORMATION

Apurva Bhasin was born in 1991 in Delhi, India. She received her BSc Honours degree (2012) and M.Sc in Chemistry (2014) from the Institute for Excellence in Higher Education, Bhopal, India. Her master's project at Nirmal University, India, focused on biochemistry techniques involving enzyme screening, purification, and characterization. She holds two-years of experience with developing thermoresponsive polymeric hydrogels as a research assistant at Amity University, India. She is currently pursuing her Ph.D. at the University of California, Irvine under

the supervision of Dr. Reginald Penner, and her research focuses on the development of virus-based impedimetric biosensors for the rapid detection of cancer biomarkers.

Nicholas P. Drago, born July, 1996 in Palos Heights, IL, earned a B.S. degree in Chemistry from Elmhurst University in 2018. He is a graduate student studying Physical Chemistry at University of California, Irvine. He conducts research in Dr. Reginald Penner's lab, with a focus on polymer-based point-of-care electrochemical biosensing.

Sudipta Majumdar was born on January 12, 1977 in India. He is a Senior Research Scientist in the Weiss laboratory focusing on engineering proteins. Dr. Majumdar completed his PhD under the supervision of Nobel Laureate Robert Huber and Tad A. Holak at the MPI for Biochemistry, Munich and did his postdoc at the UC Irvine. His research interests include phage display and characterization of proteins. He has worked in Sanofi (India) as a Scientist (R&D). He has received the Crystal Structure Award for his contributions in solving structure of proteins. Recently, he was awarded the outstanding reviewer accolade by Elsevier.

Emily C. Sanders received her BS in Biochemistry at Western Washington University in 2016. She is currently a PhD candidate in Chemistry at University of California, Irvine under the supervision of Prof. Gregory Weiss. Her research interests are interdisciplinary in nature and broadly revolve around the interface of molecular biology and polymer chemistry.

Gregory A. Weiss was born in New York City, USA in 1970. He earned a B.S. degree from the University of California, Berkeley, where he conducted research with Paul Bartlett, and a Ph.D. from Harvard University, working with Stuart L. Schreiber. Awarded a NIH Kirschstein NRSA from the NIH, he pursued post-doctoral studies at Genentech with Jim Wells. In 2000, he joined the faculty at University of California, Irvine where his laboratory focuses on combinatorial biology, continuous flow biosynthesis, and bioelectronics. Tenured in 2006, he is currently a full Professor and Vice Chair in the Department of Chemistry.

Reginald M. Penner (b. 1960, Canada) is an electrochemist who received a B.A. degree in Chemistry and Biology from Gustavus Adolphus College and a PhD with Charles Martin at Texas A&M University. He studied with Nate Lewis as a postdoctoral fellow at Stanford and Caltech and joined the Department of Chemistry at University of California, Irvine in 1990. His research group investigates electrochemical methods for preparing nanomaterials, and studies applications for these nanomaterials in sensors, energy storage, and photonic devices. Presently, he is Chancellor’s Professor and Associate Dean for Research and Innovation in the School of Physical Sciences at UCI.

ACKNOWLEDGEMENTS: R.M.P. gratefully acknowledges the financial support of this work by the National Science Foundation, through contract CBET-1803314. R.M.P. and G.A.W. both gratefully acknowledge support from the National Cancer Institute of the NIH (1R33CA206955-01), PhageTech Inc (PHAGE-203015), and the Chao Family Comprehensive Cancer Center, UC Irvine. FE-SEM data were acquired using the instrumentation of the LEXI (lexi.eng.uci.edu/) and IMRI (ps.uci.edu/imri/) facilities at UCI. We thank the healthy urine donors who consented to have their urine used in this study through UCI clinical protocol IRB HS# 2014-1758

Literature References:

(1) Yang, L. M. C.; Tam, P. Y.; Murray, B. J.; McIntire, T. M.; Overstreet, C. M.; Weiss, G. A.; Penner, R. M. Virus Electrodes for Universal Biodetection. *Anal. Chem.* **2006**, *78*, 3265–3270.

(2) Donavan, K. C.; Arter, J. A.; Weiss, G. A.; Penner, R. M. Virus-Poly(3,4-Ethylenedioxythiophene) Biocomposite Films. *Langmuir* **2012**, *28*, 12581–12587.

(3) Bhasin, A.; Ogata, A. F.; Briggs, J. S.; Tam, P. Y.; Tan, M. X.; Weiss, G. A.; Penner, R. M. The Virus Bioresistor: Wiring Virus Particles for the Direct, Label-Free Detection of Target Proteins. *Nano Lett.* **2018**, *18*, 3623–3629.

(4) Bhasin, A.; Sanders, E. C.; Ziegler, J. M.; Briggs, J. S.; Drago, N. P.; Attar, A. M.; Santos, A. M.; True, M. Y.; Ogata, A. F.; Yoon, D. V; et al. Virus Bioresistor (VBR) for Detection of Bladder Cancer Marker DJ-1 in Urine at 10 PM in One Minute. *Anal. Chem.* **2020**, *92*, 6654–6666.

(5) Smith, G. P.; Petrenko, V. A. Phage Display. *Chem. Rev.* **1997**, *97*, 391–410.

(6) Smith, G. P. Phage Display: Simple Evolution in a Petri Dish (Nobel Lecture). *Angew. Chemie Int. Ed.* **2019**, *58*, 14428–14437.

(7) Winter, G.; Milstein, C. Man-Made Antibodies. *Nature*. January 1991, pp 293–299.

(8) Marks, J. D.; Hoogenboom, H. R.; Bonnert, T. P.; McCafferty, J.; Griffiths, A. D.; Winter, G. By-Passing Immunization: Human Antibodies from V-Gene Libraries Displayed on Phage. *J. Mol. Biol.* **1991**, *222*, 581–597.

(9) Li, Z.; Chen, G. Y. Current Conjugation Methods for Immunosensors. *Nanomaterials* **2018**, *8*, 278–283.

(10) Petrenko, V. A.; Vodyanoy, V. J. Phage Display for Detection of Biological Threat Agents. *J. Microbiol. Methods* **2003**, *53*, 253–262.

(11) Petrenko, V. A. Landscape Phage as a Molecular Recognition Interface for Detection Devices. *Microelectronics J.* **2008**, *39*, 202–207.

(12) Nanduri, V.; Sorokulova, I. B.; Samoylov, A. M.; Simonian, A. L.; Petrenko, V. A.; Vodyanoy, V. Phage as a Molecular Recognition Element in Biosensors Immobilized by Physical Adsorption. *Biosens. Bioelectron.* **2007**, *22*, 986–992.

(13) Yang, L.-M. C.; Diaz, J. E.; McIntire, T. M.; Weiss, G. A.; Penner, R. M. Covalent Virus Layer for Mass-Based Biosensing. *Anal. Chem.* **2008**, *80*, 933–943.

(14) Yang, L.-M. C.; Diaz, J. E.; McIntire, T. M.; Weiss, G. A.; Penner, R. M. Direct Electrical Transduction of Antibody Binding to a Covalent Virus Layer Using Electrochemical Impedance. *Anal. Chem.* **2008**, *80*, 5695–5705.

(15) Zhang, S.; Huang, F.; Liu, B.; Ding, J.; Xu, X.; Kong, J. A Sensitive Impedance Immunosensor Based on Functionalized Gold Nanoparticle-Protein Composite Films for Probing Apolipoprotein A-I. *Talanta* **2007**, *71*, 874–881.

(16) Yan, F.; Sadik, O. A. Enzyme-Modulated Cleavage of DsDNA for Supramolecular Design of Biosensors. *Anal. Chem.* **2001**, *73*, 5272–5280.

(17) Yan, F.; Sadik, O. A. Enzyme-Modulated Cleavage of DsDNA for Studying Interfacial Biomolecular Interactions. *J. Am. Chem. Soc.* **2001**, *123*, 11335–11340.

(18) Ruan, C.; Yang, L.; Li, Y. Immunobiosensor Chips for Detection of Escherichia Coli O157:H7 Using Electrochemical Impedance Spectroscopy. *Anal. Chem.* **2002**, *74*, 4814–4820.

(19) Liu, J.; Tian, S.; Neilsen, P. E.; Knoll, W. In Situ Hybridization of PNA/DNA Studied Label-Free by Electrochemical Impedance Spectroscopy. *Chem. Commun.* **2005**, No. 23, 2969–2971.
(20) Yang, L.; Li, Y.; Erf, G. F. Interdigitated Array Microelectrode-Based Electrochemical Impedance Immunosensor for Detection of Escherichia Coli O157:H7. *Anal. Chem.* **2004**, *76*, 1107–1113.
(21) Taggart, D. K.; Yang, Y.; Kung, S.-C.; McIntire, T. M.; Penner, R. M. Enhanced Thermoelectric Metrics in Ultra-Long Electrodeposited PEDOT Nanowires. *Nano Lett.* **2011**, *11*, 125–131.
(22) Xiang, C.; Kung, S.-C.; Taggart, D. K.; Yang, F.; Thompson, M. A.; Güell, A. G.; Yang, Y.; Penner, R. M. Lithographically Patterned Nanowire Electrodeposition: A Method for Patterning Electrically Continuous Metal Nanowires on Dielectrics. *ACS Nano* **2008**, *2*, 1939–1949.
(23) Xiang, C.; Yang, Y.; Penner, R. M. Cheating the Diffraction Limit: Electrodeposited Nanowires Patterned by Photolithography. *Chem. Commun.* **2009**, No. 8, 859.
(24) Lamboy, J. A.; Arter, J. A.; Knopp, K. A.; Der, D.; Overstreet, C. M.; Palermo, E. F.; Urakami, H.; Yu, T.-B.; Tezgel, O.; Tew, G. N.; et al. Phage Wrapping with Cationic Polymers Eliminates Nonspecific Binding between M13 Phage and High p I Target Proteins. *J. Am. Chem. Soc.* **2009**, *131*, 16454–16460.
(25) Arter, J. A.; Taggart, D. K.; McIntire, T. M.; Penner, R. M.; Weiss, G. A. Virus-PEDOT Nanowires for Biosensing. *Nano Lett.* **2010**, *10*, 4858–4862.
(26) Arter, J. A.; Diaz, J. E.; Donavan, K. C.; Yuan, T.; Penner, R. M.; Weiss, G. A. Virus–Polymer Hybrid Nanowires Tailored to Detect Prostate-Specific Membrane Antigen. *Anal. Chem.* **2012**, *84*, 2776–2783.
(27) Menke, E. J.; Thompson, M. A.; Xiang, C.; Yang, L. C.; Penner, R. M. Lithographically Patterned Nanowire Electrodeposition. *Nat. Mater.* **2006**, *5*, 914–919.
(28) Chang, S. S. Overview of Prostate-Specific Membrane Antigen. *Rev. Urol.* **2004**, *6 Suppl 10*, S13-8.
(29) O'Keefe, D. S.; Bacich, D. J.; Heston, W. D. W. Comparative Analysis of Prostate-Specific Membrane Antigen (PSMA) versus a Prostate-Specific Membrane Antigen-like Gene. *Prostate* **2004**, *58*, 200–210.
(30) Diaz, J. E.; Yang, L.-M. C.; Lamboy, J. A.; Penner, R. M.; Weiss, G. A. Synthesis of a Virus Electrode for Measurement of Prostate Specific Membrane Antigen. In *Methods in molecular biology (Clifton, N.J.)*; 2009; pp 255–274.
(31) Mohan, K.; Donavan, K. C.; Arter, J. A.; Penner, R. M.; Weiss, G. A. Sub-Nanomolar Detection of Prostate-Specific Membrane Antigen in Synthetic Urine by Synergistic, Dual-Ligand Phage. *J. Am. Chem. Soc.* **2013**, *135*, 7761–7767.
(32) Donavan, K. C.; Arter, J. A.; Pilolli, R.; Cioffi, N.; Weiss, G. A.; Penner, R. M. Virus-Poly(3,4-Ethylenedioxythiophene) Composite Films for Impedance-Based Biosensing. *Anal. Chem.* **2011**, *83*, 2420–2424.
(33) Mohan, K.; Penner, R. M.; Weiss, G. A. Biosensing with Virus Electrode Hybrids. *Curr. Protoc. Chem. Biol.* **2015**, *7*, 53–72.
(34) Ogata, A. F.; Edgar, J. M.; Majumdar, S.; Briggs, J. S.; Patterson, S. V.; Tan, M. X.; Kudlacek, S. T.; Schneider, C. A.; Weiss, G. A.; Penner, R. M. Virus-Enabled

Biosensor for Human Serum Albumin. *Anal. Chem.* **2017**, *89*, 1373–1381.
(35) Tan, W. S.; Tan, W. P.; Tan, M.-Y.; Khetrapal, P.; Dong, L.; DeWinter, P.; Feber, A.; Kelly, J. D. Novel Urinary Biomarkers for the Detection of Bladder Cancer: A Systematic Review. *Cancer Treat. Rev.* **2018**, *69*, 39–52.
(36) Kumar, P.; Nandi, S.; Tan, T. Z.; Ler, S. G.; Chia, K. S.; Lim, W.-Y.; Bütow, Z.; Vordos, D.; De laTaille, A.; Al-Haddawi, M.; et al. Highly Sensitive and Specific Novel Biomarkers for the Diagnosis of Transitional Bladder Carcinoma. *Oncotarget* **2015**, *6*, 13539–13549.
(37) Rivnay, J.; Inal, S.; Salleo, A.; Owens, R. M.; Berggren, M.; Malliaras, G. G. Organic Electrochemical Transistors. *Nat. Rev. Mater.* **2018**, *3*, 17086.
(38) Wang, N.; Yang, A.; Fu, Y.; Li, Y.; Yan, F. Functionalized Organic Thin Film Transistors for Biosensing. *Acc. Chem. Res.* **2019**, *52*, 277–287.
(39) Lin, P.; Yan, F.; Chan, H. L. W. Ion-Sensitive Properties of Organic Electrochemical Transistors. *ACS Appl. Mater. Interfaces* **2010**, *2*, 1637–1641.
(40) Li, H.; Shi, W.; Song, J.; Jang, H.-J.; Dailey, J.; Yu, J.; Katz, H. E. Chemical and Biomolecule Sensing with Organic Field-Effect Transistors. *Chem. Rev.* **2019**, *119*, 3–35.
(41) Gao, N.; Zhou, W.; Jiang, X.; Hong, G.; Fu, T.-M.; Lieber, C. M. General Strategy for Biodetection in High Ionic Strength Solutions Using Transistor-Based Nanoelectronic Sensors. *Nano Lett.* **2015**, *15*, 2143–2148.

Figures:

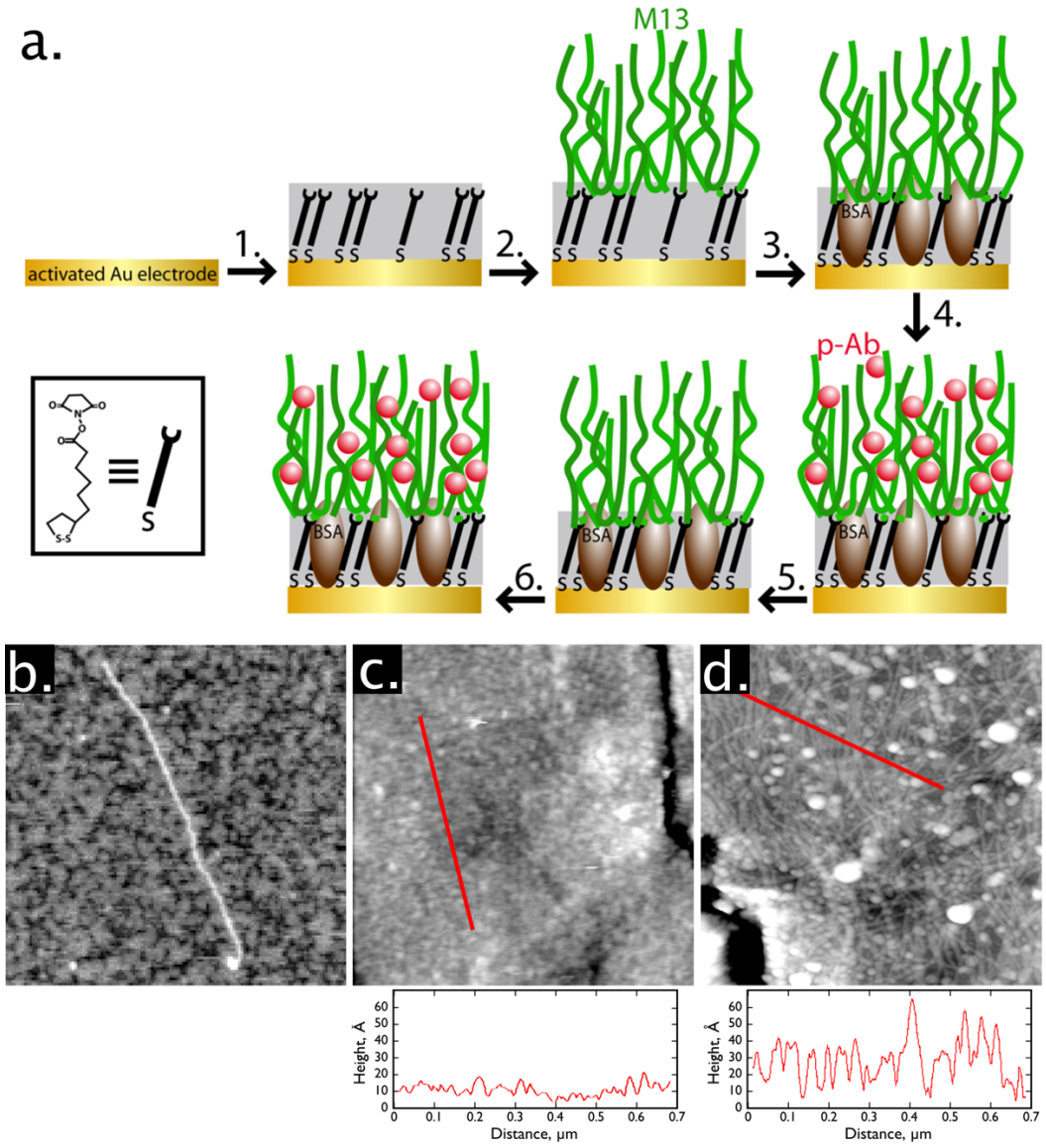

Figure 1 – The covalent virus surface (CVS). a). Stepwise assembly (steps 1−3) and functionalization (steps 4−6) of the CVS. (b-d) Noncontact mode AFM images (1 μm × 1 μm). (b) A single M13 virion on mica, (c) A self-assembled monolayer (SAM) of *N*-hydroxy-succinimide thioctic ester on gold after exposure to BSA. No virus particles were attached to this surface. (d) A functional CVS consisting of a SAM of *N*-hydroxysuccinimide thioctic ester (NHS-TE) on gold, reacted with M13 to produce covalent attachment, and exposed to BSA (Figure 1, step 3). After Ref.[13]

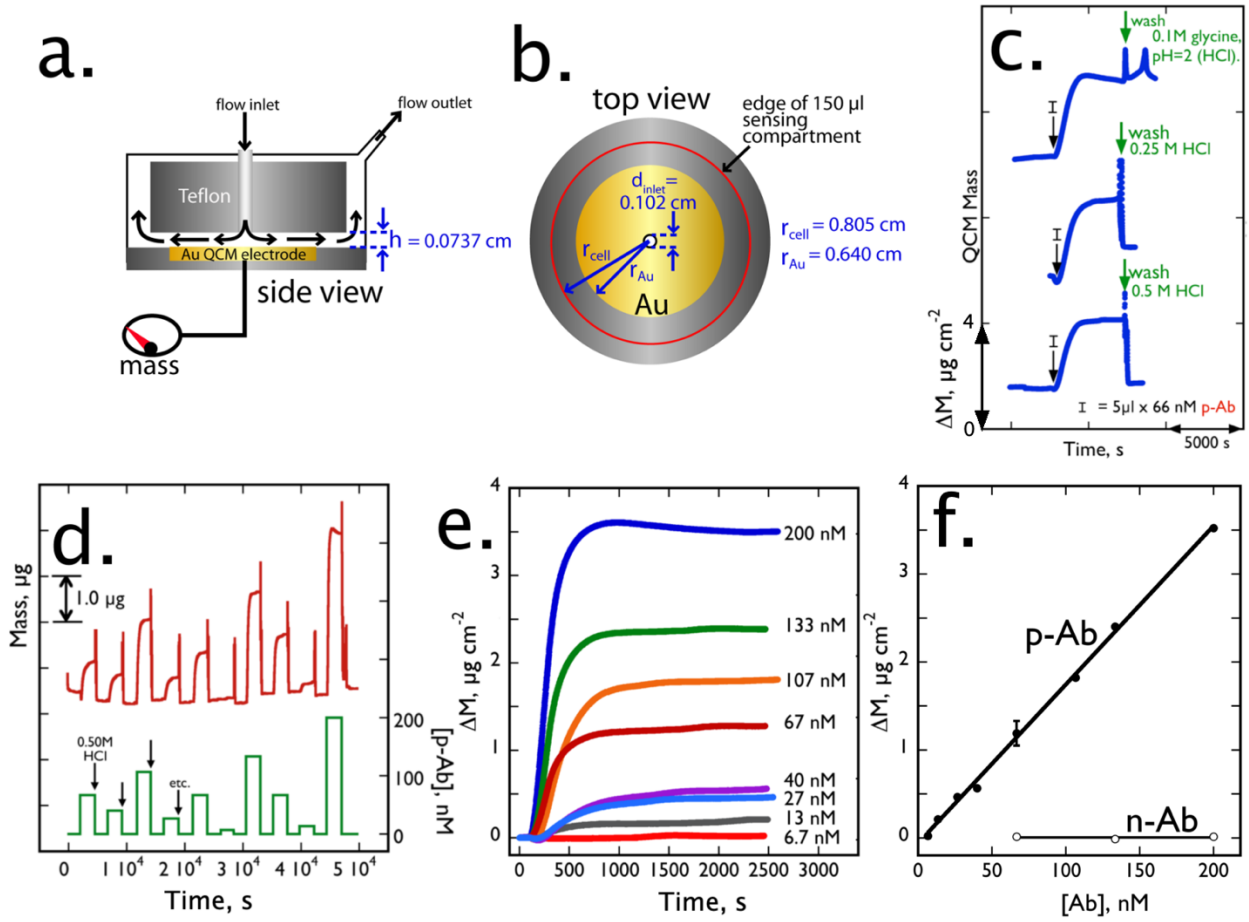

Figure 2 – QCM investigations of the CVS. a,b) Schematic diagram of the QCM and flow cell. c). QCM evaluation of the efficacy of three wash solutions as indicated. d,e). d) Plot of mass *versus* time for the exposure of a CVS to doses of p8-Ab, ranging in concentration from 6.6 to 200 nM. e). Same data as shown in (d), but normalized to the same injection time to precisely show relative heights of these transients. f) Plot of maximum mass change versus p8-Ab concentration for the data shown in (d,e). The mass change was proportional to the concentrations of injected p8-Ab (R^2 = 0.997) and yielded a sensitivity of 0.018 (μg cm^{-2})/nM and a limit of detection (LOD) of 6.6 nM. After Ref.[13]

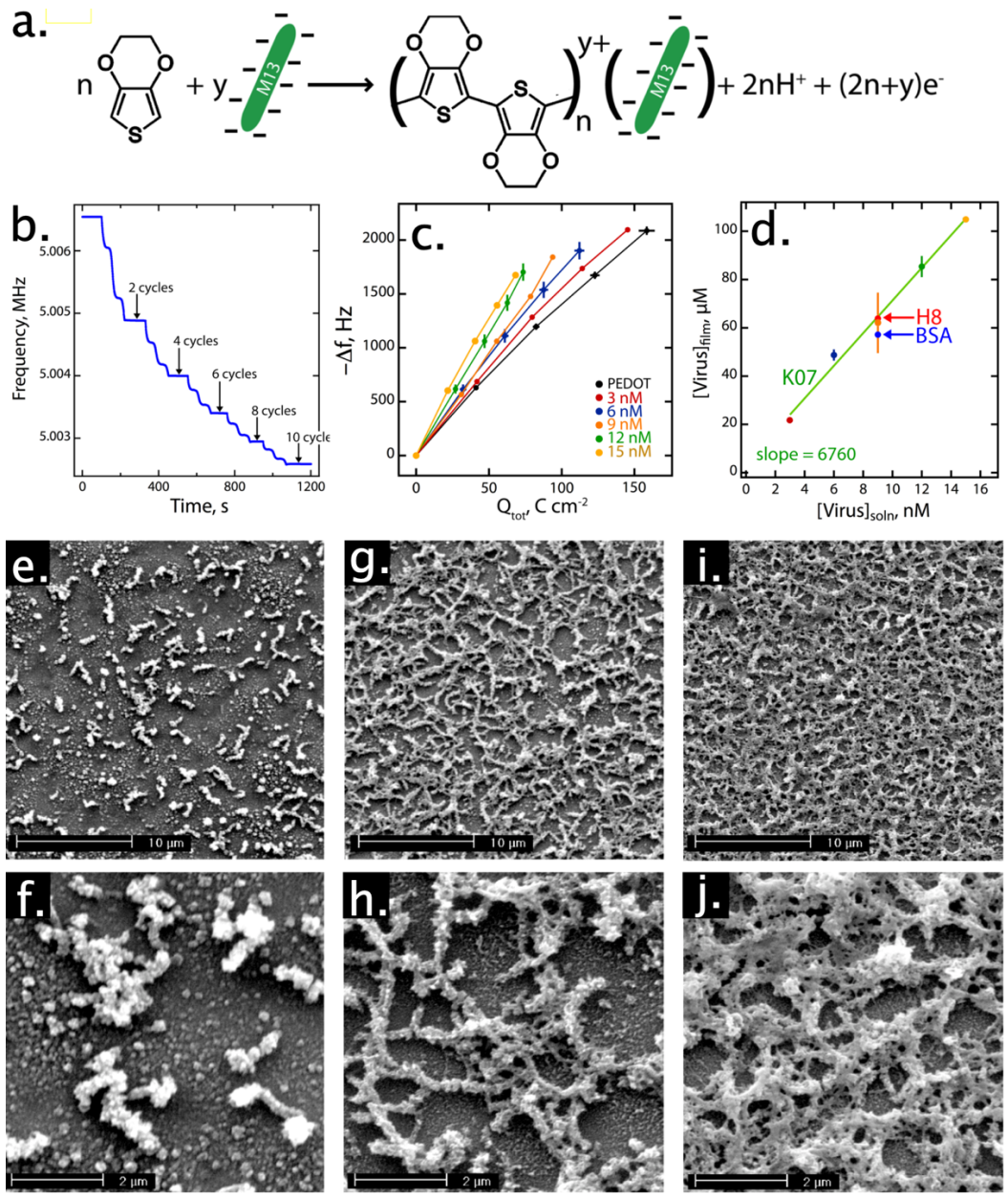

Figure 3 – Electrodeposition of a virus-PEDOT bioaffinity layer. a). The virus-PEDOT electrodeposition reaction, b). QCM analysis of virus-PEDOT electrodeposition shows increased mass loading as a decrease in frequency. c) Frequency change *versus* deposition charge, Q_{tot}, for QCM measurements. d) Calibration curve showing the linear correlation of the virus concentration within the PEDOT film (vertical axis) *versus* the concentration of virus in solution. (e-j). Topography of virus-PEDOT films imaged by scanning electron microscopy. Films were prepared from solutions containing virus particles at three concentrations: (e,f) $[virus]_{soln}$ = 3 nM, (g,h) $[virus]_{soln}$ = 9 nM, and (I,j) $[virus]_{soln}$ = 15 nM. After Ref.[2]

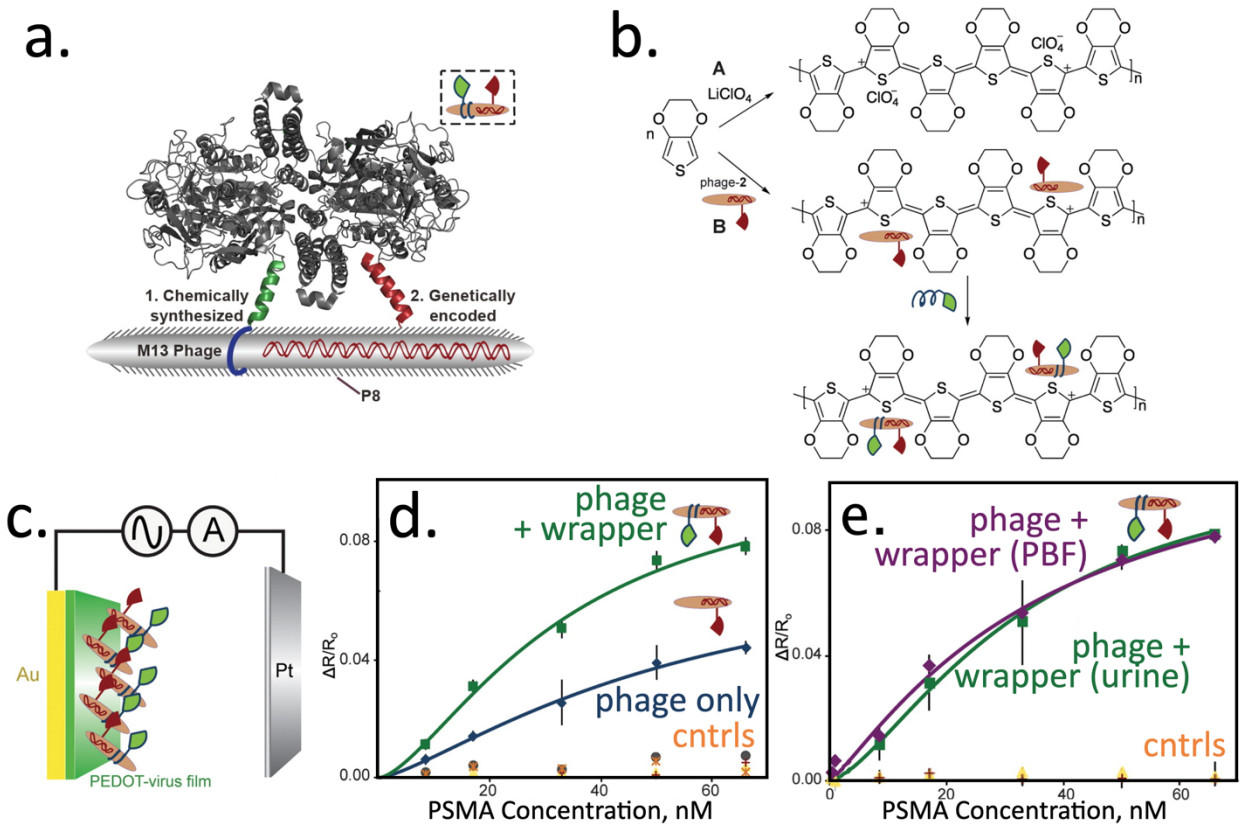

Figure 4 – PSMA Detection in Synthetic Urine Using Synergistic, Dual-Ligand Phage. a) Schematic diagram of bidentate binding to PSMA by KCS-1, (green) and genetically encoded peptide, (red). Simultaneous binding by these two ligands provides higher apparent affinity to PSMA. b). Polymerization reactions of EDOT in the presence of: (top) $LiClO_4$ or (center)) PSMA-binding phage, and (bottom) PSMA-binding phage and exposure to the wrapper KCS-1 (Green), c). Schematic diagram of the biosensing experiment. (d) $\Delta R/R_o$ of the film increases with the PSMA concentration. e). Comparison of PSMA detection in synthetic urine (green) with detection in PBF buffer (purple). After Ref.[31]

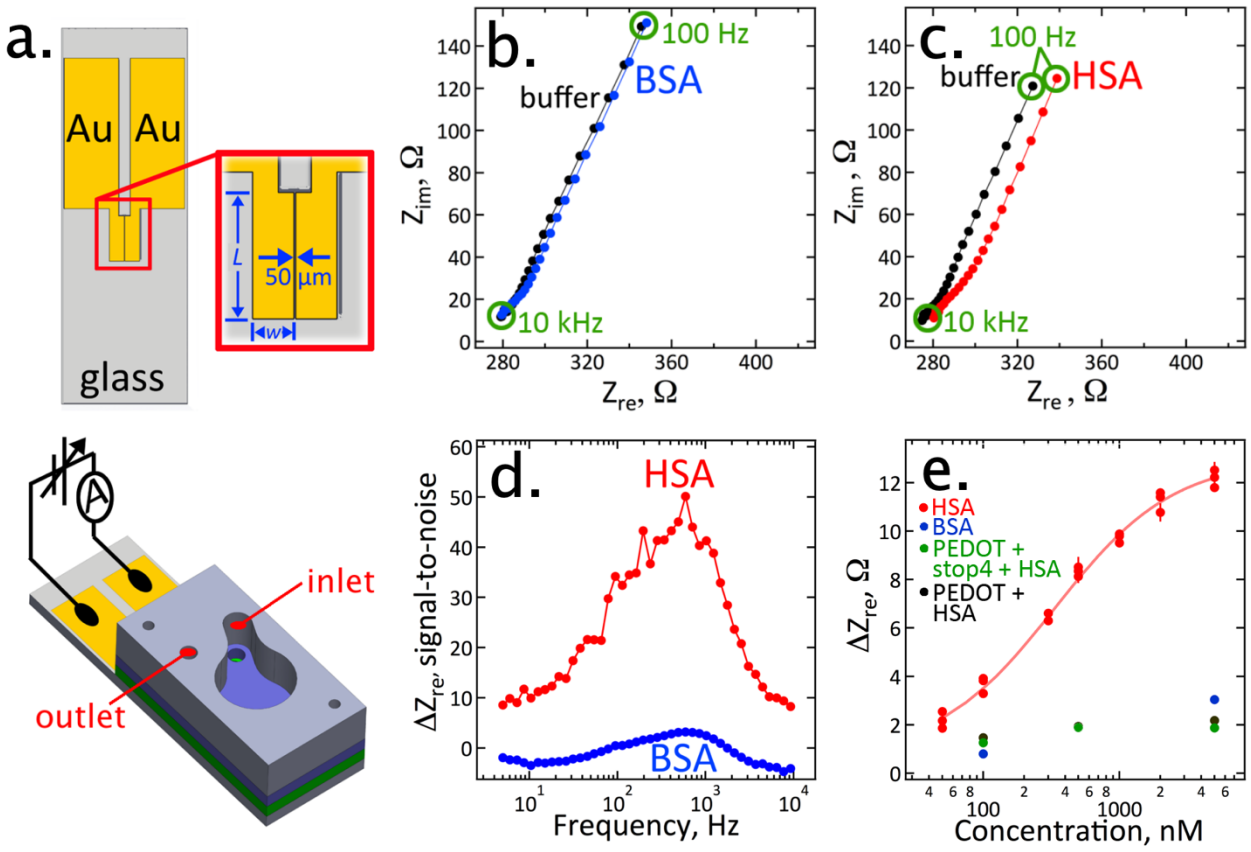

Figure 5 – The Two-Sided Biosensor: A Monolithic Biosensor for Human Serum Albumin (HSA). a). Engineering diagram of two electrode virus-PEDOT biosensor. b,c) Nyquist plots (Z_{im} vs. Z_{re}) for a control protein (BSA) and HSA. d). Signal-to-noise *versus* frequency plot for HSA and BSA. e). ΔR_{re} *versus* HSA concentration calibration curve. Controls for BSA, and off-virus binding also shown. After Ref.[3]

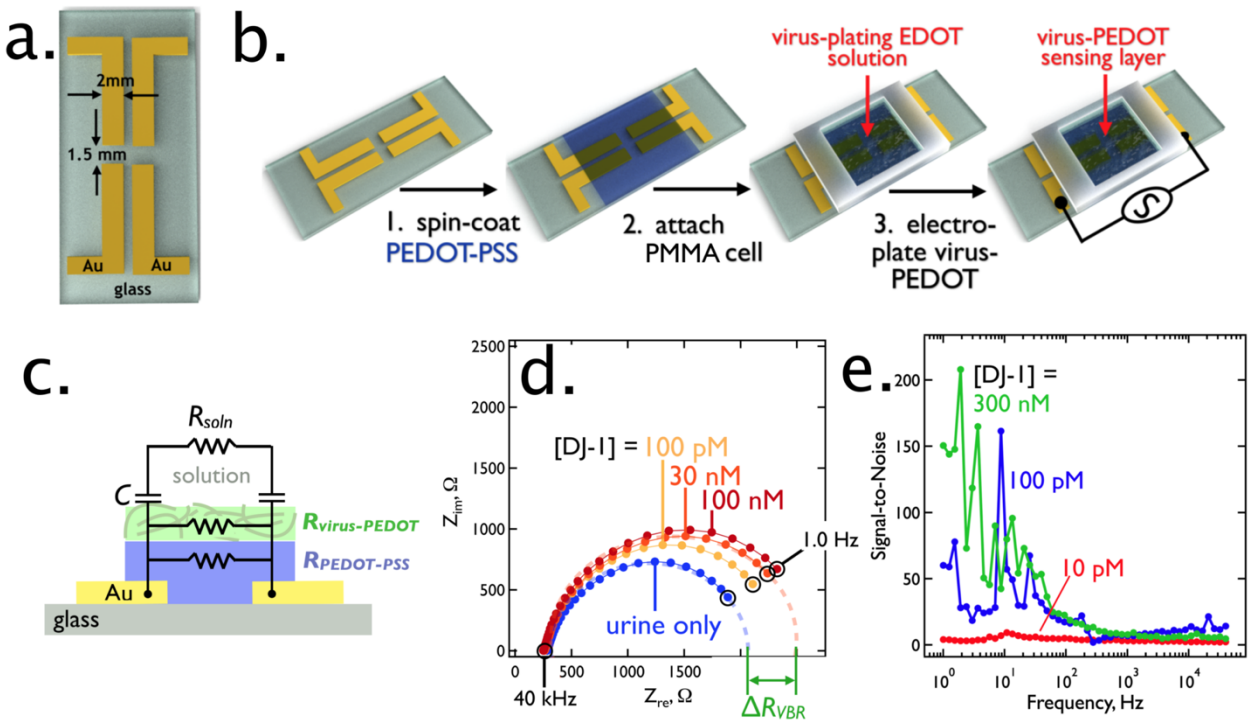

Figure 6 – The Virus BioResistor (VBR). a) VBRs are constructed on a 10 mm glass chip with patterned gold electrodes. b). Three processing steps provide for the deposition of a PEDOT-PSS layer by spin-coating from solution (Step 1), the attachment of a PMMA cell (Step 2), and the electrodeposition of a virus-PEDOT layer (Step 3). c). The electrical response of the VBR is modeled by three parallel resistors and a solution/channel capacitance. d). This circuit produces a semi-circular Nyquist plot for which the high frequency impedance (40 kHz) approximates the solution resistance ($Z_{re} \approx R_{soln}$), and the low frequency impedance is dominated by the parallel resistance imposed of the two film resistors, $Z_{re} \approx Z_{VBR}$. Z_{VBR} increases with the concentration of target protein present in the solution phase. e). The VBR circuit maximizes signal-to-noise (S/N) at low frequencies, and can exceed 100 at high protein concentrations. After Ref.[4]

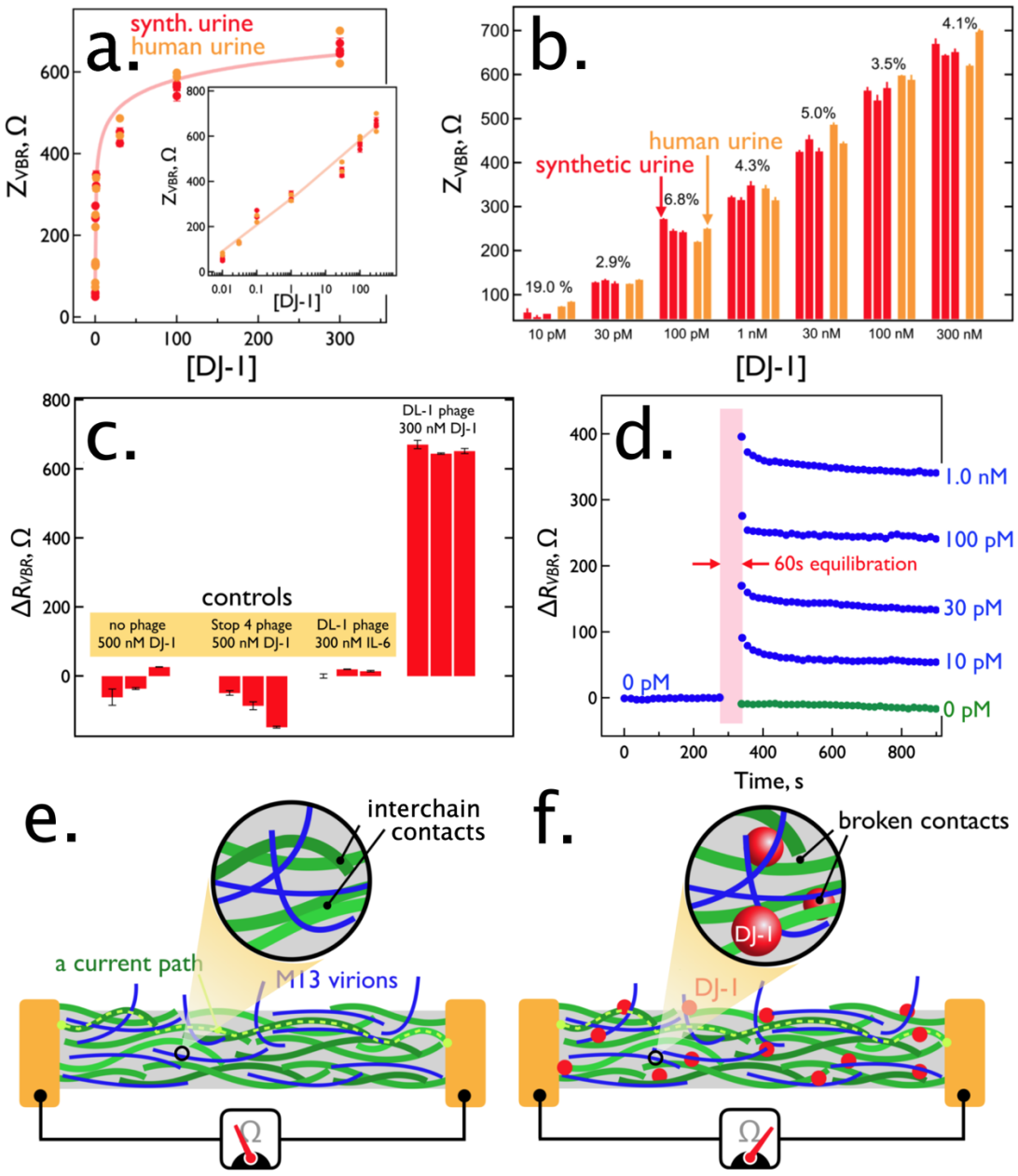

Figure 7 – Rapid Quantitation of DJ-1 in Urine. a,b) Correlation of VBR signal against DJ-1 concentration in urine and synthetic urine. c). Comparison of DJ-1 signal at 300 nM with three controls, d). VBR signal versus time for the exposure of five VBRs to aliquots of DJ-1 in synthetic urine. e,f). Proposed mechanism for VBR signal transduction. After Ref. [4]